

EFFECTS OF OPEN-CHANNEL GEOMETRY ON FLOW PATTERN IN A 90° JUNCTION^{*}

S. MOHAMMADIUN¹, S. A. A. SALEHI NEYSHABOURI^{2**}, GH. NASER³, H.
PARHIZKAR⁴ AND H. VAHABI⁵

¹Hydraulic Structural Eng., Faculty of Civil and Environmental Eng., Tarbiat Modares University, I. R. of Iran

²Faculty of Civil and Environmental Eng. and Water Eng. Research Center, Tarbiat Modares University, I. R. of Iran
Email: salehi@modares.ac.ir

³School of Eng. Faculty, University of British Columbia, Canada

⁴Aerospace Eng., Amirkabir University of Technology, I. R. of Iran

⁵Mechanical Eng., University of Tehran, I. R. of Iran

Abstract– Open-channel junctions have a broad application in civil and environmental engineering. Formation of a low-pressure zone with recirculating flow (high sedimentation) accompanied by a high-velocity zone (high erosion) is the most characteristic feature of flow in junctions. A large number of researches have been performed to study the complexity of the flow in junctions in open-channel flows. In this research, four new geometrical modifications, based on streamlinization concept, are investigated to understand their effects on reducing the sedimentation and erosion potential in a 90° open-channel junction. First, the numerical model was validated based on previous experimental studies. Then, effects of the mentioned modifications were evaluated and some efficiency measures were devised to improve their performance. The results show that employing the proposed geometrical modifications improves the flow pattern significantly via eliminating the recirculation zone and reducing the maximum flow velocity after the junction. Thereby a comprehensive reduction in sedimentation and erosion potential is produced as well as contracting the stagnation zone.

Keywords– Open-channel junction, geometrical modification, numerical model, sedimentation, erosion

1. INTRODUCTION

Open-channel junctions are common structures in hydraulic and environmental engineering. The interaction between the main and branch flows causes the main flow to be diverted toward the opposite bank of junction and this interaction creates a separation zone at the downstream corner of the junction. Formation of a three dimensional (3D) separation zone with lower pressure immediately near the branch-side bank is one of the most distinctive characteristics of a flow in open-channel junctions. The recirculating flow in this low-pressure zone not only prepares a suitable space for sedimentation which is a common problem in hydraulic structures that can block intakes or junctions [1], but also increases the velocity near the opposite bank of the main channel and its bed and thereby leads to local erosion. Reducing the sedimentation in recirculation zone and eliminating the erosion near the opposite wall of the channel are two major concerns for designers.

Numerous experimental, numerical and analytical studies were conducted to first explore the flow structure in the junctions and then to reduce the sedimentation and erosion rates. Best and Reid [2] studied the general flow characteristics of junctions to investigate effective parameters on the size of separation

*Received by the editors April 3, 2014; Accepted December 2, 2014.

**Corresponding author

zone. They also investigated the effects of various connecting angles between main and branch channels, ranging from 15° to 90° , on flow pattern and shape index of the recirculation zone. Ramamurthy *et al.* [3] derived a relation between the depth of flow at the junction and the ratio of the branch discharge to the total discharge on the basis of the momentum principle. Weber *et al.* [4] explored the flow pattern of combining flows in a 90° open channel via performing a comprehensive experimental study and provide valuable data giving three velocity components, turbulence stresses, and water surface mappings. Huang *et al.* [5] implemented an extended numerical study of combining flows in open-channel junctions using the 3D turbulent model and investigated the effect of junction angle. Using the 3D $k-\omega$ turbulence model and the Reynolds averaged Navier-Stokes equations (RANS), Zhang *et al.* [6] explored the effect of discharge ratio (ratio of the flow in upstream main channel to the total flow downstream) on the shape of separation zone, the cross-sectional mean flow angle, and the contraction coefficient for a 90° equal-width open-channel junction flow. Developing a hybrid RANS-based large eddy simulation (LES) model, Zeng and Li [7] simulated flow in an open-channel T-junction. Their results were more accurate when compared to those from RANS approach. Bonakdari *et al.* [8] developed a two-phase, Eulerian, CFD (Computational Fluid Dynamics) model in a 30° junction to investigate the effect of relative flow rate on the size of recirculation zone. The volume of fluid (VOF) scheme is used to capture the free surface.

Shamloo and Pirzadeh [9] provided detailed application of the FLUENT software and Reynolds Stress Modeling (RSM) turbulent model in simulation of lateral intake flows. Li and Zeng [10] focused on effects of vegetation on fluid flow in an open channel junction. A 3D RANS (Reynolds Averaged Navier–Stokes) equation model is implemented in their work to investigate the flow phenomena in the channel junctions with or without vegetation. Ting *et al.* [11] solved the Reynolds averaged Navier-Stokes equations for the 90° equal-width open-channel junction flow, while using 3D $K-\omega$ model to obtain the mean flow pattern and the secondary currents. Their validated model is then applied to investigate the effect of the discharge ratio on the shape of separation zone, the cross-sectional mean flow angle and the contraction coefficient. Using 2D numerical model, right angled channel confluence flow was investigated by Baghlani and Talebbeydokhti [12].

Detailed hydrodynamics of junction flow is found to be complex [12] and there exist a number of parameters that characterize the flow pattern. These include the size, shape, slope, and angle between two channels, Froude and Reynolds numbers. Simplified theoretical models are not capable of taking all these variables into account. Moreover, studies based on physical models are expensive. The need to obtain more details from velocity field for the design of junctions has recently prompted the development of 3D numerical methods which do not invoke many simplifying assumptions and proved to be reliable.

Geometry modification at junction of main and branch channels is investigated thoroughly in this research to evaluate its effect on flow structure improvement via reducing the size of recirculation zone and maximum velocity after the junction. A primary objective of the present study is to investigate the effect of eliminating the sharp junction's corners on flow pattern in the main channel. Following that, a new geometrical modification based on the concept of streamlined body is introduced and its influence on flow structure is investigated. In contrast to changing the connection angle, these modifications, introduced in this research, have not been studied in much detail in previous studies. 3D CFD model is employed to explore the effects of the abovementioned methods on flow structure which leads the flow to a less eroding condition. Numerical validation was performed based on Weber *et al.*'s. [4] extensive experimental study on 90° open-channel junction flows. Finally, the optimum condition is proposed.

2. NUMERICAL MODELING

The governing equations for open-channel flows are incompressible and steady-state Reynolds Averaged Navier-Stokes (RANS) equations in Cartesian coordinate system [13]:

$$\frac{\partial U_i}{\partial x_i} = 0 \quad (1)$$

$$\rho U_j \frac{\partial U_i}{\partial x_j} = -\frac{\partial P}{\partial x_i} + \frac{\partial}{\partial x_j} (2\nu S_{ji} - \overline{\rho u_i u_j}) \quad (2)$$

where x_i = spatial coordinates, i and $j=1, 2, 3$; U_i =mean velocity in the x_i -direction; t =time; g =gravitational acceleration; ρ =density of fluid; P =pressure; ν =molecular viscosity; $\overline{u_i u_j}$ = terms in Reynolds stress tensor, and S_{ji} is the strain tensor.

In order to take the effects of turbulence into account, Reynolds Stress Modeling (RSM) has been selected. Since the RSM turbulence model accounts for the effects of streamline curvature, swirl, rotation, and rapid changes in strain rate in a more rigorous manner than other classical models, it is expected to be more accurate for complex flows and capture the secondary flows and separation zones in ducts [13]. Abandoning the isotropic eddy-viscosity hypothesis, the RSM closes the Reynolds-averaged Navier-Stokes equations by solving transport equations for the Reynolds stresses, together with an equation for the dissipation rate. This means that seven additional transport equations are required in 3D flows.

FLUENT [13] is a powerful and flexible general-purpose CFD software used for modeling flow, turbulence, heat transfer, and reactions. Various physical models allow accurate analysis on finite volumes for a wide range of fluid-related problems - from airflow over an aircraft wing to combustion in a furnace, from oil platforms to flow through channels [13]. This software uses the finite volume method to solve the governing equations.

Approximation of the convection term is handled by the second order upwind schemes (SOU) in various models of the present study. Moreover, the pressure-velocity coupling is achieved using the SIMPLE-C algorithm.

This research employed the experimental study performed by Weber *et al.* [4] to verify the results of numerical model. As indicated in Fig. 1, the test includes the flow in a sharp-edged, 90° junction of a main and branch channel with identical cross section (0.91×0.51 m). All dimensions were normalized by the channel width, $W=0.914$ m. The normalized coordinates are $X^*=x/W$, $Y^*=y/W$, and $Z^*=z/W$.

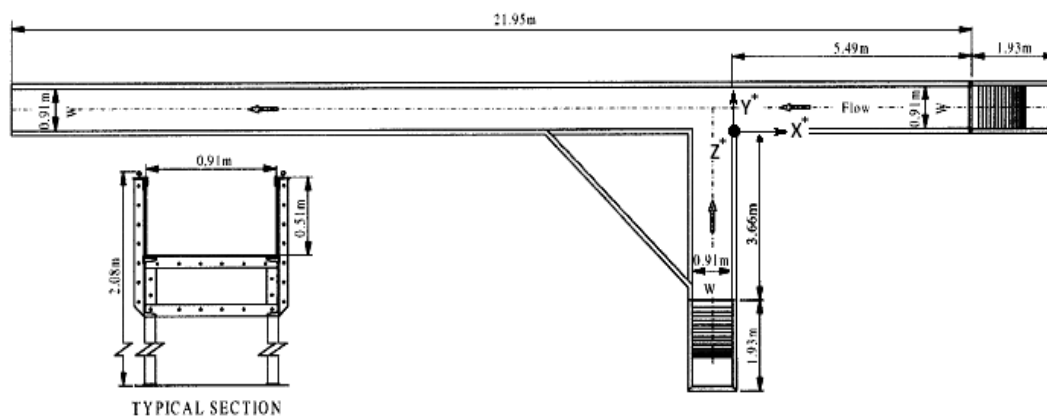


Fig. 1. Experimental flume layout of Weber *et al.* [3]

Free-surface elevation was not known before the computation, thus the inflow velocity distributions can no longer be prescribed as fully developed [14]. Following Huang *et al.*, the main channel upstream of the junction was lengthened to 10.973 m (12 W), and the side channel was prolonged to 9.144 m (10 W), so that the uniform velocity distributions were prescribed at the inflow boundaries.

Appropriate boundary conditions were applied for velocity and pressure at the inlet of main and branch channels as well as the outlet of main channel, respectively. All essential boundary data such as velocities and turbulent quantities were obtained from Weber *et al.* [4] Furthermore, a steady state analysis was performed to investigate the flow pattern in operating condition. Following grid independency study, a total number of $60 \times 40 \times 30$ (x, y, z) and $200 \times 40 \times 30$ cells were chosen for upstream and downstream parts in the main channel, respectively.

As well, $55 \times 40 \times 30$ cells were used for branch channel. Furthermore, a finer mesh in junction region guaranteed a robust result (Fig. 2).

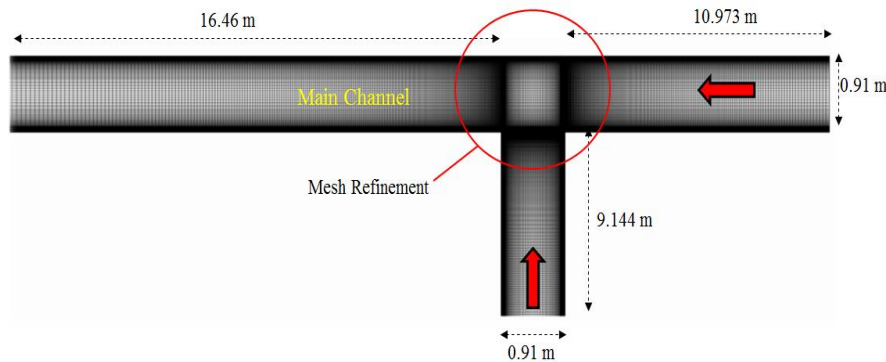


Fig. 2. Numerical Grid geometry of the junction

Although the open-channel flow originally consists of two phases of water and air, the substitution of simple one-phase simulation for its two-phase counterpart is in great demand. This replacement is possible just in case the difference between maximum and mean elevation of water free surface is negligible. Leschziner and Rodi [14] concluded that performing a simple, one-phase simulation with rigid free water surface is acceptable, provided that the relative difference between maximum and mean elevation of water free surface is less than 10%. In this case, symmetric boundary condition is applicable on the water free surface. To investigate the accuracy of one-phase simulation, both one and two-phase analyses were performed and the results were compared. Free surface in the one-phase analysis assumed that a free-slip boundary occurred without normal velocities (symmetric boundary condition), while the volume of fluid (VOF) scheme was employed at the free surface in the two-phase approach.

3. VERIFICATION

The experimental data of Weber *et al.* were selected for validation. The time-averaged components of velocities at each data point (Fig. 3) were normalized, using the constant tail-water average velocity $V_t = 0.628$ m/s. In this research, the discharge ratio of 0.25 was selected for validation as it generates a clearer separation zone.

The total height of channel (0.51 m) was considered in the two-phase analysis which was performed with an Eulerian approach. However, the flow depth was assumed 0.29 m and VOF scheme was employed at the free surface of water. The U^* contour at $Z^* = 0.278$ and $X^* = -2$ is shown in Fig. 4 for the experimental Weber *et al.* [4] and numerical (two-phase) results. Clearly, a recirculation zone after the junction in numerical analysis (Zone I) is verified by the experimental study. Low negative and positive velocities are the most characteristic features of this region. Formation of the recirculation zone causes an increase in water velocity in Zone II due to the contraction in cross section. As flow passes through the main channel, the flow pattern changes gradually to a fully developed one after Zone III. In contrast to the

abovementioned similarities, a high gradient velocity near the walls (Zone IV) is not observable in the experimental study (Fig. 4D), due to the relatively rough grid in the experimental work (Fig. 3).

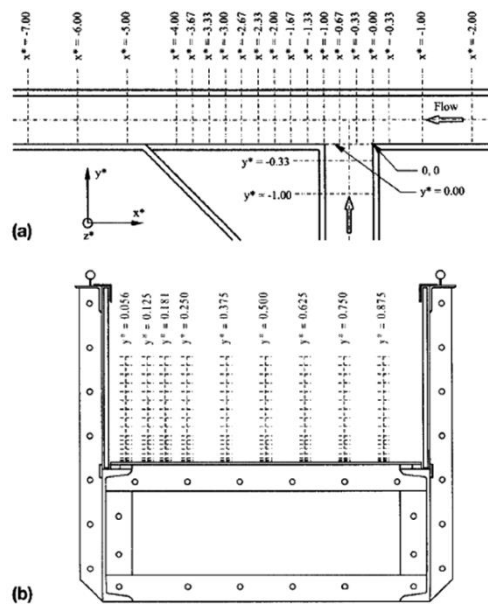


Fig. 3. Location of: (a) Cross sections; (b) Flow velocity measurement

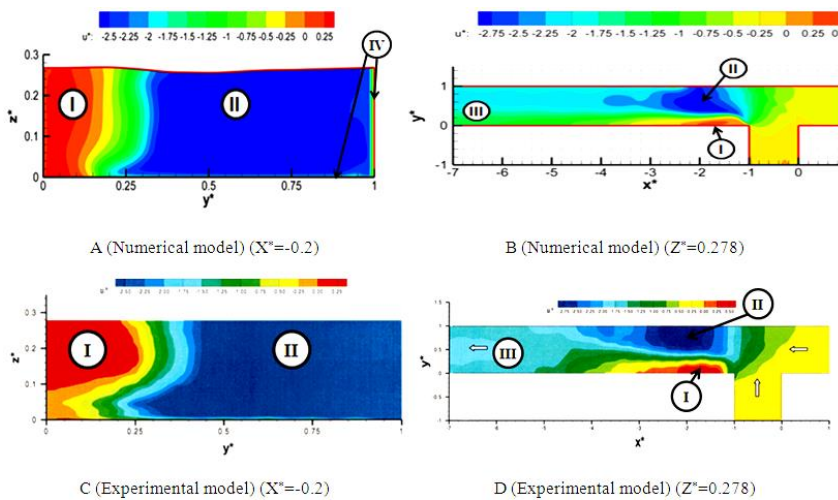


Fig. 4. U^* contours at $Z^*=0.278$ and $X^*=-2$

For a more quantitative comparison, the numerical and experimental results for absolute maximum U^* versus X^* (after the junction) are shown in Fig. 5. The figure reveals a rapid increase in the maximum absolute U^* (until $X^*=-2$), followed by a slight decline. Neglecting the suspicious discontinuity in experimental data at $X^*=-1.5$, the maximum U^* difference between numerical and experimental results is estimated at less than 3%.

Implementing a one-phase analysis instead of two-phase one, improves computational efficiency significantly. Therefore, as the maximum difference between maximum and mean elevation of water free surface is less than $0.06 \cdot h$ (with h as the flow depth), this replacement was investigated more.

In contrast with two-phase simulation, variations of water free surface elevation were not taken into account in one-phase analysis. Thus the one-phase model water depth was constant (0.29 m, equal to $Z^*=0.32$ in Weber *et al.* study). Figure 6 reveals the results of one-phase analysis for contours of U^* at

$Z^*=0.278$ and $X^*=-2$. Profiles of Zones I and II in one-phase simulation are somehow different from their counterparts in two-phase analysis (Fig. 4).

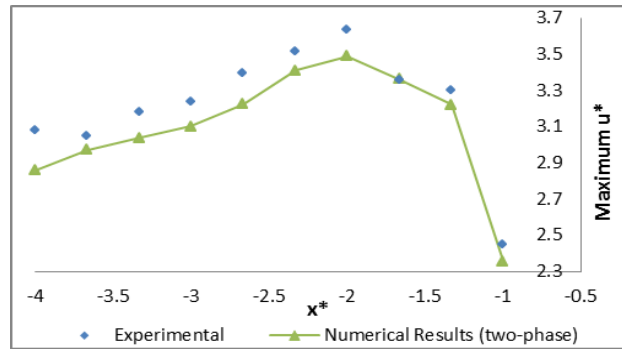


Fig. 5. Variation of the absolute maximum U^* along the channel after junction

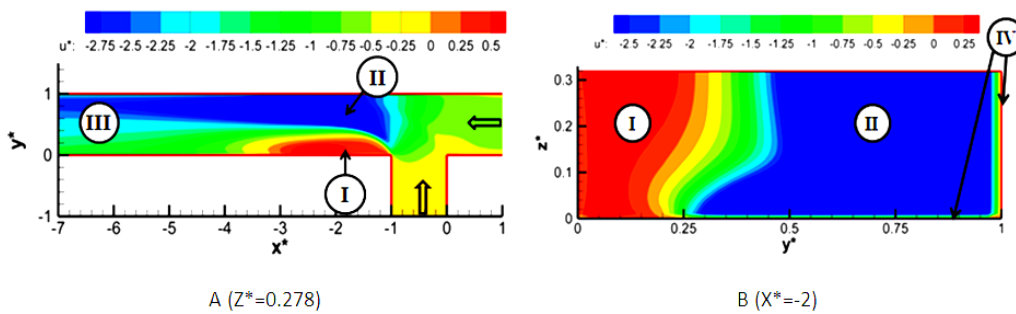


Fig. 6. U^* contour at $Z^*=0.278$ and $X^*=-2$ in numerical one-phase analysis

The variations of absolute maximum U^* versus X^* after the junction, for one-phase simulation and experimental study, are shown in Fig. 7. The figure shows reasonable agreement between the two sets of results (maximum difference is less than 7%).

Figure 8 compares one-phase numerical and experimental results for U^* velocities at different locations ($Y^*=0.25, 0.375, 0.5, 0.625$) along the flow depth at $X^*=-2$ which shows a reasonable agreement. Figure 8 (A) depicts the variation of U^* at $X^*=-2$ and $Y^*=-0.25$. As can be seen, since the upper part of curve is located in the recirculation zone, U^* values are considerably small and positive. The U^* profile changes slightly and remains unchanged at locations away from the recirculation zone (Fig. 8 C and D).

Overall, the discrepancy between one and two-phase numerical results in predicting the maximum U^* after the junction (Figs. 5 and 7) is less than 7%. Interestingly, the U^* contours (Figs.4 and 6) and U^* variation along the flow depth (Fig. 8) in numerical (one-phase) and experimental studies are noticeably similar. Hence, one-phase analysis is implemented in the rest of this research.

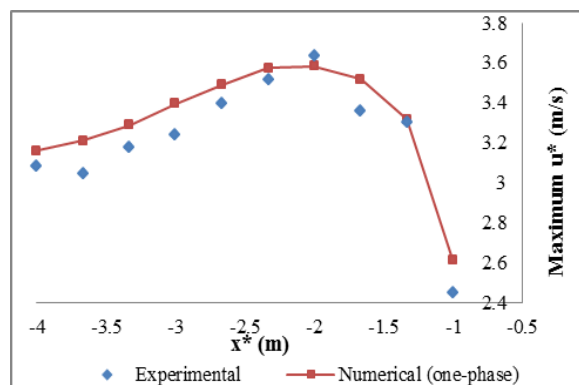


Fig. 7. Variation of the absolute maximum U^* along the channel after junction

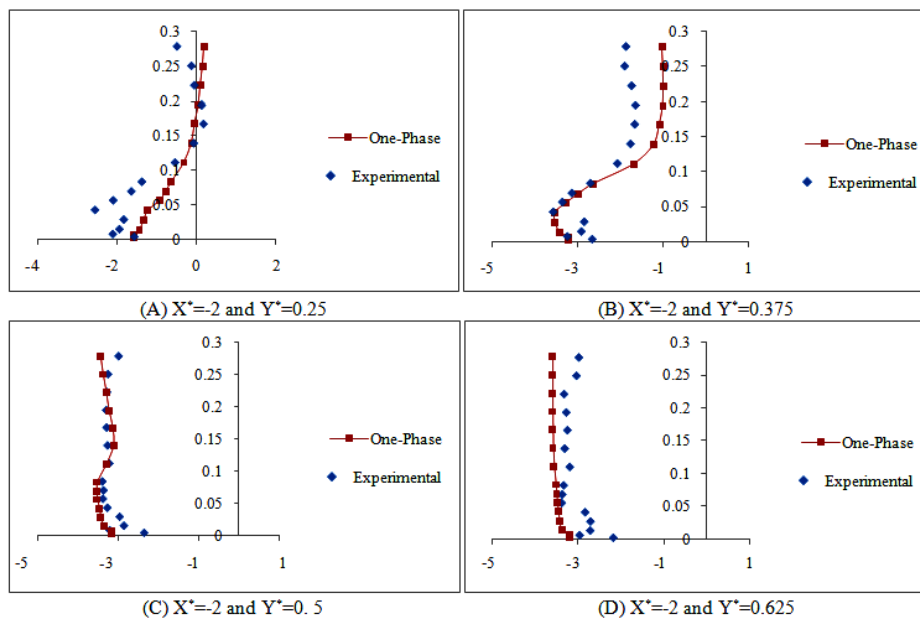


Fig. 8. Variation of U^* along the flow depth at $X^* = -2$

4. METHODS TO IMPROVE FLOW CONDITIONS

Although the direction of branch flow changes as it enters the main channel, the flow is not capable of adjusting its direction with a downward sharp, 90° corner (Corner No.1 in Fig. 9) and thus it is unable to flow tangentially along the Wall No. 2. The region between the flow path and Wall No. 2 is a suitable region for recirculation. This recirculating flow leads to sedimentation in the mentioned region as well as increasing the flow velocity and thus erosion between recirculation zone and Wall No. 1 (Fig. 9) via contracting the flow cross section (Fig. 10).

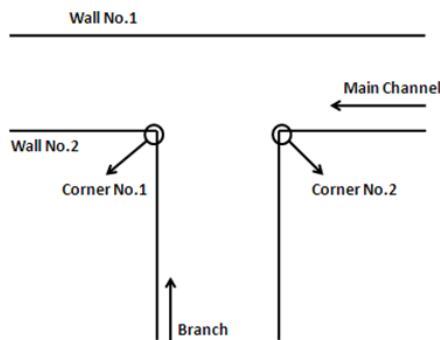


Fig. 9. Different parts of a junction

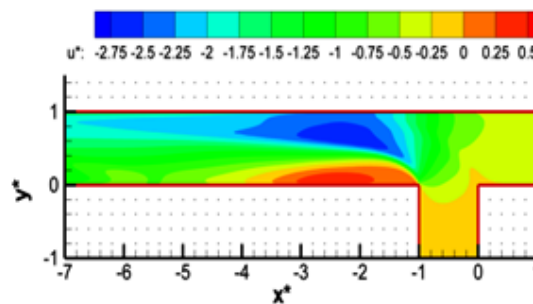


Fig. 10. Recirculation zone after the junction and velocity increase above it

In this research, four different geometrical modifications (denoted as cases in Fig. 11) were modeled at the junction to achieve an in-depth understanding of their effects on flow pattern.

Moreover, the optimal geometry was introduced and its effect on contracting the recirculation zone and reducing the maximum velocity after the junction were evaluated.

a) Case No. 1 (Fig. 11. A): Employing two identical arcs at two corners of the junction

Designing the junction with two arcs with identical radii was the first geometrical modification investigated in this study to eliminate the recirculation zone. Various numerical models consisting of two identical arcs with different radii were prepared. Normalized arc radii of 0.273, 0.383, 0.547, and 1 were

employed to investigate the effects of changing arc radius on flow pattern. All radii were normalized by the channel width ($W=0.914$ m) and shown by R^* . The discharge ratio of 0.25 and the main flow U^* of 0.2325 were used in all models.

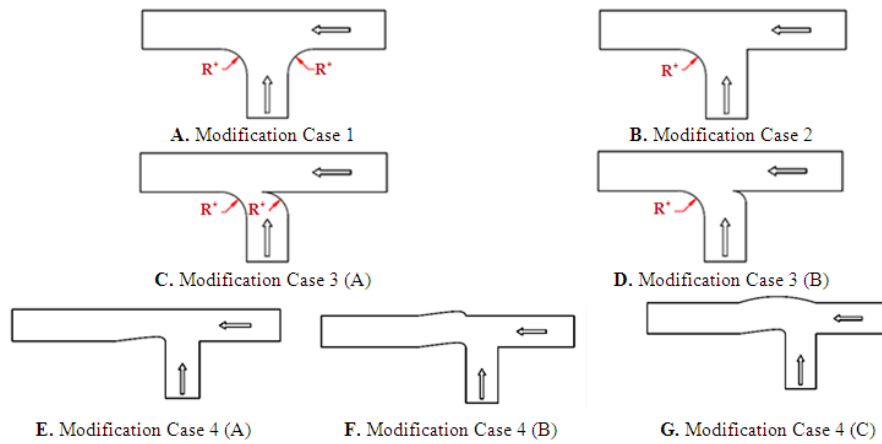


Fig. 11. Geometry modifications investigated at the junction

Figure 12 depicts the U^* contours at the junction consists of two identical arcs with normalized radius (R^*) of 0.273.

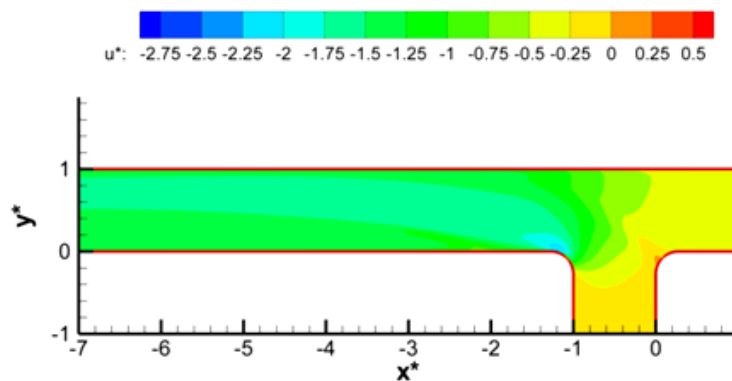


Fig. 12. Contours of U^* in junction consists of two arcs with $R^*=0.273$

Compared with Fig. 10, a considerable reduction in velocity gradient after the junction is shown. Clearly, employing two arcs with $R^*=0.273$ eliminates the recirculation zone after the junction completely.

Employing an arc at Corner No. 1 (Fig. 9) not only expands the flow cross section at $X^*=-1$ and thus reduces the flow velocity in this section, but also leads the water to flow tangentially along the arc which causes a noticeable reduction in recirculation zone. Interestingly, any reduction in recirculation width causes a considerable decline in flow velocity by increasing the flow cross section. Velocity evaluations in different models reveals that the maximum U^* after the junction in each case occurs at the location where the arc finishes. If an arc with a larger radius is substituted for the previous smaller one, the flow cross section after the junction increases more at each X^* which is located within the range of the radius with a smaller arc. Therefore, higher reduction in velocity would be obtainable in case arcs with larger radii employed. Considering some vertical lines between $X^*=-1$ and $X^*=-2$ in Fig. 13, it would be obvious that the velocity reduces as the arc radius increases. Furthermore, as mentioned before, the presence of the arc at Corner No. 1 weakens the recirculation strength via forcing the water to flow tangentially along the corner curve. Increasing the arc radius causes the water to flow more tangentially along the curve and causes more reduction in the recirculation strength. Therefore, as can be seen in Fig. 13, the maximum flow velocity in the channel reduces as the arc radius increases. Furthermore, raising the arc radius

decreases the centrifugal force on branch flow as it passes tangentially along the arc which leads to a considerable reduction in the radial component of branch flow velocity adjacent to the arc. This velocity reduction along the arc radius causes the branch flow to move more tangentially and reduces its radial displacement; hence the branch flow cross section increases as it enters the junction and thus the branch velocity reduces.

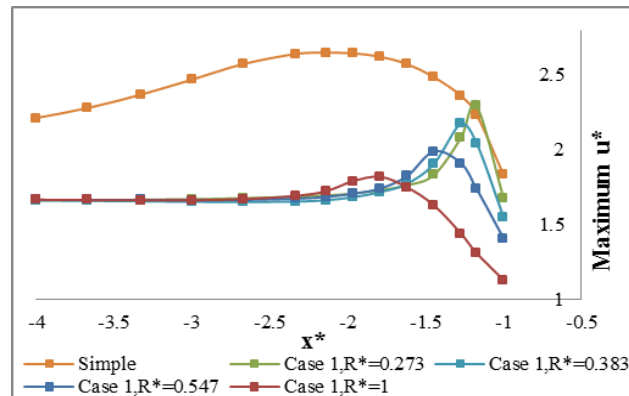


Fig. 13. Changes in maximum U^* after the junction in models consist of two arcs

In case the arc radius in Corner No. 1 is not large enough, effects of the arc at location where it finishes are negligible in comparison with simple junction (the corner without arc); while its influence on reducing the flow velocity after the arc is considerable. Figure 13 illustrates that, compared with simple junction, changes in the maximum U^* at $X^*=-1.273$ are negligible in case an arc with $R^*=0.273$ is employed. On the contrary, using an arc with $R^*=0.383$ in Corner No. 1 causes a 9% reduction in maximum U^* at $X^*=-1.383$. Likewise, 25% (at $X^*=-1.547$) and 31% (at $X^*=-2$) velocity reduction would be obtainable provided that arcs with $R^*=0.547$ and $R^*=1$ are employed, respectively.

Maximum U^* and thus maximum erosion occur at $X^*=-2$ in simple channel. Figure 13 illustrates that the presence of arcs, regardless of their radius at both corners of the junction, causes a noticeable reduction in flow velocity at $X^*=-2$. As can be seen from the figure, maximum U^* reduces 39% and 31% occur with $R^*=0.383$ and $R^*=1$, respectively.

In contrast with the simple junction in which flow pattern is thoroughly influenced by presence of recirculation zone and the maximum U^* reduces slowly along the X^* after $X^*=-2$ (Fig. 13), maximum U^* declines dramatically after the location where arc finishes and reaches a constant value, 1.65, in models with modified geometry at Corner No. 1. This rapid reduction in velocity is important in design of flumes.

Improving the flow pattern due to increasing the arc radius continues up to full elimination of the recirculation zone and reduces the maximum velocity after Corner No. 1. However, increasing the radius of the arc at Corner No. 2 (Fig. 9) causes an expansion in flow cross section and thus a velocity reduction before the junction. Reducing the main flow velocity and momentum at Corner No. 2 produces a stagnation zone (Fig. 14), which expands due to increasing the radius of the arc.

b) Case No. 2 (Fig. 11 B): Employing an arc at Corner No. 1 of the junction

In order to eliminate the stagnation zone near Corner No. 2, accompanied by a reduction in size of the recirculation zone after Corner No. 1, the use of just one arc at Corner No. 1 was investigated. Furthermore, effects of increasing the arc radius were evaluated using four models consisting of an arc with different normalized radius of 0.273, 0.383, 0.547 and 1, respectively. The sharp (90°) angle at Corner No. 2 remained in all four models. As expected, the maximum U^* after the junction in these models (Fig. 15) is similar to their previous counterparts (Fig. 13). Moreover, Fig. 15 reveals that the maximum U^* after the junction reduces by 39% in the most appropriate model ($R^*=1$).

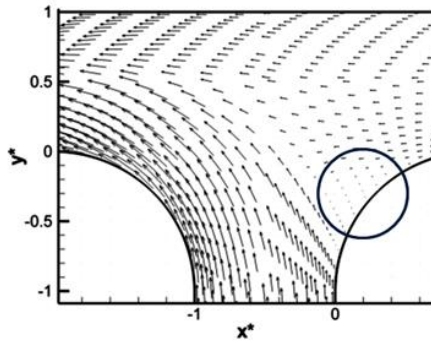
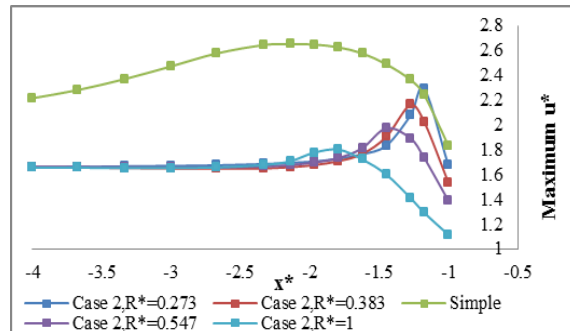


Fig. 14. Stagnation zone near the corner No. 2

Fig. 15. Charges in maximum U^* after the junction in models consist of one arc

Corner No. 2 is more susceptible to formation of an extended stagnation zone as the arc radius (in Corner No. 1) increases and branch flow is diverted towards it (Fig. 14).

In comparison with the junction, which consists of two identical arcs, employing just one arc (at Corner No. 1) decreases the size of stagnation zone.

c) Case No. 3 (Fig. 11 c and d): Employing two parallel arcs at two corners of the junction

As shown previously, any expansion at adjoining section of main and branch channels provides an isolated area for stagnation zone to occur; hence geometry modification in the mentioned section aimed at shrinking the stagnation zone, were investigated. Therefore two identical parallel arcs in two junction corners (Fig. 11c) was investigated. Furthermore, effects of increasing the arc radius were evaluated using four models consisting of arcs with different normalized radius of 0.273, 0.383, 0.547, and 1. However, Fig. 17 reveals that the adjoining cross section contracts and thus flow is diverted towards the Wall No. 2 (Fig. 9) as arcs radii are increased. Although the flow diversion could eliminate the recirculation zone, large velocities in this region (Zone B in Fig. 17) increase the erosion potential dramatically. Likewise, the sharp angle at Corner No. 2 may encounter much erosion. The sharp angle at Zone B diverts the velocity vectors toward the Zone A noticeably (Fig. 17) and thus moves the shear plane toward the Wall No. 2. Therefore, the velocity magnitude increases near the Wall No. 2 and decreases near the Wall No. 1. In addition to much erosion at Zone A and Zone B, formation of a small velocity region beneath the Zone B (Fig. 17b) which increases the sedimentation potential would be assumed as the other drawback of this modification.

Streamlinization mitigates the fluid pressure and erosion potential. Using this approach, the body of a structure is designed and formed according to the flow path around it. Regarding this approach to modify the junction geometry, the arc at Corner No. 2 (Fig. 11c) was replaced with a suitable curve (Fig. 11d). The region with negligible velocity near the Corner No. 2 was observed in models consisting of one arc at Corner No. 1 (Fig. 11b) to recognize the suitable streamlinized curve. Following that, a spline is fitted on the boundary of the abovementioned semi-stagnated region and finally, the junction geometry at Corner No. 2 is modified using this curve (Fig. 11d). Comparing the Figs. 17 and 18 reveals that the streamlinization of the Corner No. 2 improves the flow pattern significantly, especially near the Corner No. 1. Likewise, it likely averts the semi-stagnated region near the Corner No.2 (Fig. 18b), compared with previous modifications.

Figure 19 illustrates that increasing the radius of arcs could reduce the maximum U^* after the junction rapidly and thus eliminates the recirculation zone. Interestingly, semi-stagnated region disappeared near the corner number 2.

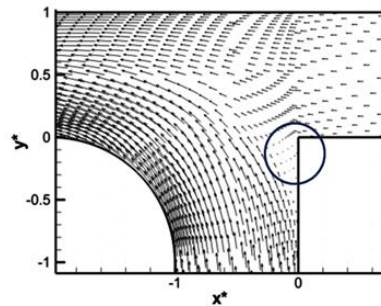


Fig. 16. Stagnation zone near the Corner No. 2

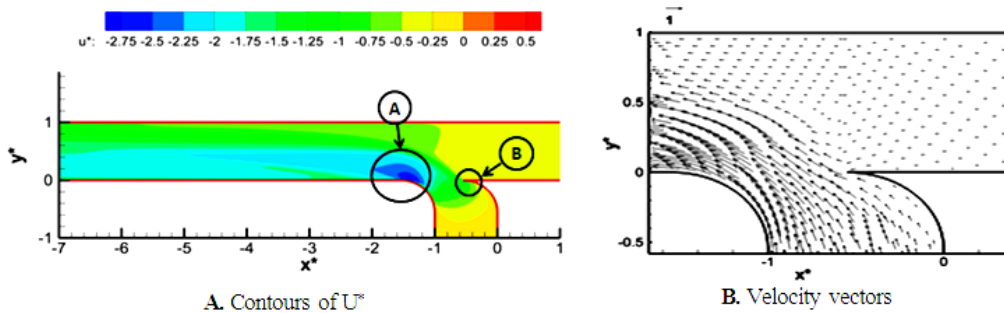


Fig. 17. Flow characteristics in a junction with two identical parallel arcs with $R^*=0.5$

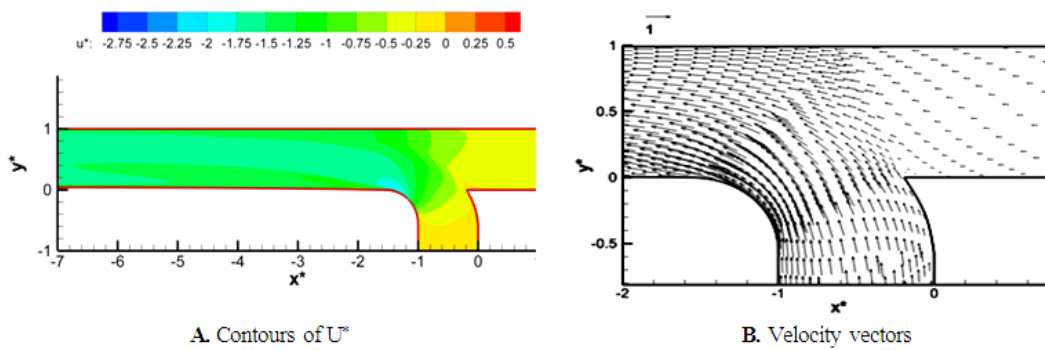


Fig. 18. Flow characteristics in a junction with an arc with $R^*=1$ and a streamlined curve at Corner No. 2

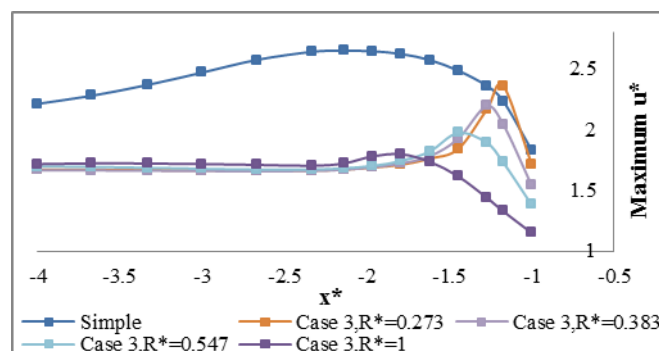


Fig. 19. Changes in maximum U^* after the junction in models consist of an arc and a streamlined curve

d) Case No. 4 (Fig. 11 e, f and g): Employing a streamlined curve at Corner No. 1

As mentioned before, the full elimination of the recirculation zone and semi-stagnated region accompanied by a significant reduction in erosion potential is obtainable with an arc at Corner No. 1 integrated with a streamlined curve at Corner No. 2; which entails employing high radii. Use of arcs with large radii may not be practical in large channels due to spatial limitations; hence performing a thorough modification in the junction was investigated to eliminate the recirculation zone without any

considerable changes in the channel size. In contrast with previous cases, elimination of semi-stagnated zones using a modified curve at Corner No. 2 (Fig. 11d), streamlinization was performed to modify the Corner No. 1 here. To do so, boundaries of the recirculation zone near the Corner No. 1 were determined in the simple model and a spline was fitted on its boundary as the channel geometry. According to the flow pattern in a simple model (Fig. 10), length and width of recirculation zone were determined as $X^*=3.84$ and $Y^*=0.26$, respectively. Therefore, the straight edge after Corner No.1 (Wall No. 2 in Fig. 9) was replaced with a spline with abovementioned sizes.

Figure 20a reveals that the streamlinization of Wall No. 2 causes the water to flow tangentially along the curve and thus eliminates the recirculation zone. However, this contraction in flow cross section increases the flow velocity and thus erosion near the Wall No. 1 and the streamlinized curved wall near the Corner No. 1. To eliminate the erosion trouble, an identical streamlinized curve was substituted for Wall No. 1 (Fig. 20b). Figure 20b shows that although employing an identical curve parallel to the first one on Wall No. 1 expands the flow cross section; it provides a convenient area for recirculating flow generation at Zone B and Zone A.

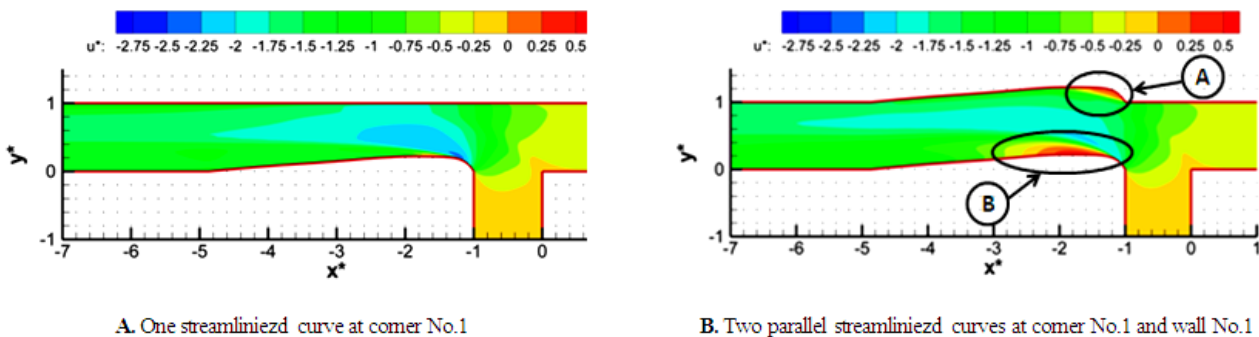


Fig. 20. Contours of U^* in two streamlinized models

Elimination of Zone B (Fig. 20b) is possible, provided that the width of the first streamlinized curve on Wall No. 2 increases (Fig. 11d). Moreover, downward increase in the length of the second curve on Wall No. 1 causes a decline in angle of corner. So the water that flows tangentially along the curve and the recirculating flow in Region A disappears.

Figure 21 shows that applying the abovementioned two streamlinized curves can resolve all hydraulic trouble after the junction. In this case, a curve with a dimensionless length of 3.12 and width of 0.41 (normalized with $W=0.91$ m) is employed on Wall No. 2, accompanied by a similar curve on Wall No. 1. However, the width of the second curve is increased and begins at $X^*=0$ (Fig. 21).

The variation of maximum U^* along the main channel after the junction in three streamlinized models is depicted in Fig. 22.

As can be seen in Fig. 22, local flow acceleration occurs just after the junction due to the presence of a streamlinized curve in Wall No. 2 which causes a contraction in the flow cross section (Case 1) compared to the size of flow cross section in simple model. As mentioned before, employing the second identical curve on Wall No. 1 expands the flow cross section and thus improves the flow pattern (Case 2). Although using both abovementioned modifications causes an increase in flow velocity immediately after the junction, their considerable influence on reducing the flow velocity after that sudden rise would be in great demand. Figure 22 illustrates that expansion of the streamlinized curve on Wall No.1 not only eliminates the separation zone in Case No. 2, but also provides a noticeable reduction in maximum U^* after the junction.

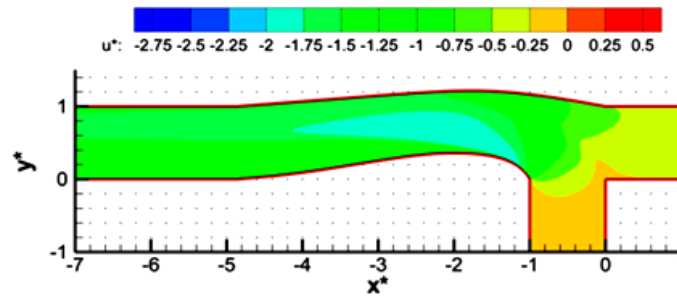


Fig. 21. Contours of U^* in model consist of two different streamlined curves

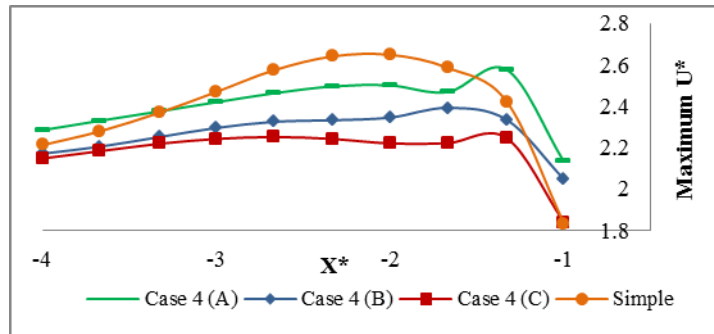


Fig. 22. Changes in maximum U^* after the junction in models consist of one or two streamlined curves

5. COMPARISON OF BEST CONFIGURATIONS

Best configuration of all cases ($R^*=1$) are compared with each other based on their effects on the variation of the maximum flow velocity along the channel width at their critical section. To do so, the critical section of each case, where the maximum velocity occurs, is identified from their relevant graph and then the maximum velocity profile across the channel width (Y^*) is extracted in the aforementioned sections. The critical section is located at $X^*=-1.792$ in case 1 to 3, while the critical section of case 4 and simple junction are located at $X^*=-1.33$ and -2 , respectively.

Figure 23 depicts the variation of maximum absolute U^* along the Y^* in the abovementioned sections. U^* changes noticeably with a steep slope between $Y^*=0.1$ and 0.45 in the simple channel. In this channel, the maximum U^* occurs in the middle part of the section, since the flow cross section contracts due to the recirculation flow near to this region. The flow velocity is negligible in the recirculation zone as well as the zones adjacent to the channel walls due to the “no-slip” condition. Likewise, a considerable change in flow velocity occurs at boundary layers near the walls.

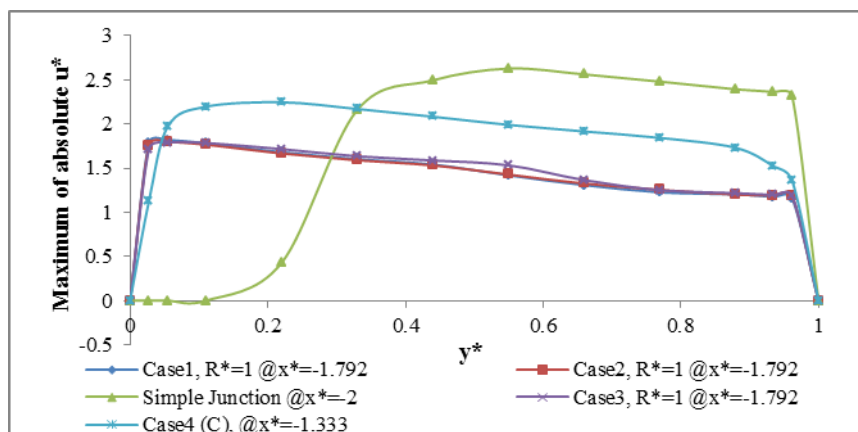


Fig. 23. Changes in maximum U^* along Y^* at critical section in each case best configuration

Figure 23 illustrates that all proposed geometrical modifications produce slight flow profiles along the channel width and eliminate the velocity gradient as well as recirculation flow out of boundary layers. Maximum U^* profile in cases 1, 2, and 3 are similar while the profile in Case 4 is somehow different. The maximum velocity reduction in Case 4 is less than the other proposed modifications.

The branch velocity magnitude and thus shear stress is larger than in the main channel before the junction. However, shear stress after the junction increases due to the flow mixture which increases the velocity magnitude. Elimination of the separation zone decreases the flow velocity and hence shear stresses after the junction, which diminishes the erosion in the channel.

The shear stress contours on walls and bottom in one of the modified (Case2, $R^*=1$) and simple flumes are depicted in Fig. 24. Shear stresses are normalized using the dynamic pressure based on flow velocity at main inlet of the channel of Weber *et al.* study (196 Pa).

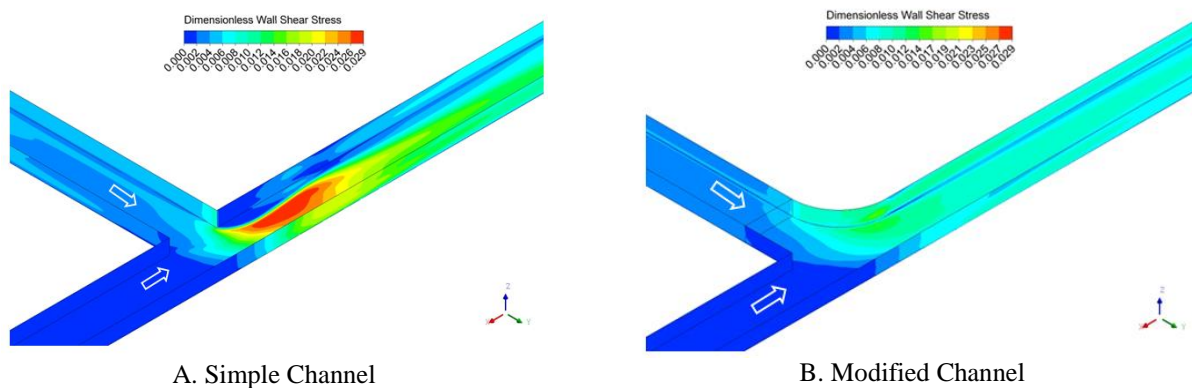


Fig. 24. Normalized shear stress in simple and modified channel

6. CONCLUSION

Flow pattern in a 90° open-channel junction were investigated in this research and some streamlinization-based geometry modifications were evaluated to improve the flow pattern and thereby reduce sedimentation as well as erosion potential. The summary of different modification performances have been depicted in Table 1. Evaluating the geometrical modifications reveals that:

Table 1. Summary of different modification performances

Type of modification	Recirculating zone	Velocity reduction	Dimension of stagnation zone	Best radius
Case No. 1	Eliminated	The Best	Large	$R^*=1$
Case No. 2	Eliminated	The Best	Medium	$R^*=1$
Case No. 3 (A)	Eliminated	Weak	Eliminated	$R^*=1$
Case No. 3 (B)	Eliminated	The Best	Small	$R^*=1$
Case No. 4 (A)	Eliminated	Weak	Large	-
Case No. 4 (B)	Diminished	Good	Large	-
Case No. 4 (C)	Eliminated	Very Good	Large	-

- Full elimination of the separation zone and thus sedimentation is possible with an arc at the downward corner of the junction. Moreover, this arc has a considerable effect on reducing the maximum flow velocity which causes a noticeable reduction in erosion potential. While it may extend the stagnation area adjacent to upward corner of the junction.

- The sharp-angle upstream corner of the junction could be modified based on streamlinization concept to prevent the formation of a stagnation area. Employing an arc identical to the one used at the downstream corner of the junction is not suggested.
- Implementing a streamlinized curve at the near-bank wall of the junction accompanied by a longer one on the opposite wall of the main channel is a suitable method for eliminating the recirculation zone and sedimentation when enough space for employing arcs is not available around the junction.
- Employing a curve with radius equal to the channel width, on the downstream edge of the junction, results in full elimination of the recirculation zone as well as a considerable reduction in flow velocity and thus shear stress after the junction which reduces the erosion in this zone.

REFERENCES

1. Talebbeydokhti, N. & Naghshineh, A. (2004). Flushing sediment through reservoirs. *Iranian Journal of Science & Technology Transactions of Civil Engineering*, Vol. 28, No. 1, pp. 119-136.
2. Best, J. L. & Reid, I. (1984). Separation zone at open-channel junctions. *Journal of Hydraulic Engineering*, Vol. 110, No. 11, pp. 1588-1594.
3. Ramamurthy, A. S., Carballada, L. B. & Tran, D. M. (1988). Combining open channel flow at right angled junctions. *Journal of Hydraulic Engineering*, Vol. 114, No. 12, pp. 1449-1460.
4. Weber, L. J., Schumate, E. D. & Mawer, N. (2001). Experiments on flow at a 90° open-channel junction. *Journal of Hydraulic Engineering*, Vol. 127, No. 5, pp. 340-350.
5. Huang, J., Weber, L. J. & Lai, Y. G. (2002). Three-dimensional numerical study of flows in open-channel junctions. *Journal of Hydraulic Engineering*, Vol. 128, No. 3, pp. 268-280.
6. Zhang, T., Xu, W. & Wu, C. (2009). Effect of discharge ratio on flow characteristics in 90° equal-width open-channel junction. *Journal of Hydrodynamics*, Ser. B, Vol. 21, No. 4, pp. 541-549.
7. Zeng, C. & Li, C. W. (2010). A hybrid RANS-LES model for combining flows in open-channel T-Junctions. *Journal of Hydrodynamics*, Ser. B, Vol. 22, No. 5, pp. 154-159.
8. Bonakdari, H., Lipeme-Kouyi, G. & Wang, X. (2011). Experimental validation of CFD modeling of multiphase flow through open channel confluence. *World Environmental and Water Resources Congress, ASCE, California, USA*, pp. 2176-2183.
9. Shamloo, H. & Pirzadeh, B. (2008). Investigation of characteristics of separation zones in T-Junctions. *WSEAS, Transactions on Mathematics*, Vol. 7, No. 5, pp. 303-312.
10. Li, C. W. & Zeng, C. (2009). 3D Numerical modeling of flow divisions at open channel junctions with or without vegetation. *Advances in Water Resources*, Vol. 32, pp. 49-60.
11. Zhang, T., Xu, W. L. & Wu Chaoand, Z. (2009). Effect of discharge ratio on flow characteristics in 90° equal-width open-channel junction. *Journal of hydrodynamics*, Vol. 21, No. 4, pp. 541-549.
12. Baghlani, A. & Talebbeydokhti, N. (2013). Hydrodynamics of right-angled channel confluences by a 2D numerical model. *Iranian Journal of Science & Technology Transactions of Civil Engineering*, Vol. 37, No. 2, pp. 271-283.
13. ANSYS-FLUENT. (2006) FLUENT 6.3 User's Guide [online]. FLUENT Documentation, Fluent Inc. Available from http://aerojet.engr.ucdavis.edu/fluenthelp/html/ug/main_pre.htm
14. Leschziner, M. A. & Rodi, W. (1979). Calculation of strongly curved open channel flow. *Journal of the Hydraulics Division*, Vol. 105, No. 10, pp. 1297-1314.